Synthesis and Electrical Behavior of Sodium Doped Monoclinic $SrSiO_3$

Mohd Najim
Department of Electrical and Electronic Engineering, College of Engineering, University of Jeddah, Saudi Arabia
mngalib@uj.edu.sa (corresponding author)

Received: 5 April 2023 | Revised: 11 June 2023 | Accepted: 26 June 2023

Licensed under a CC-BY 4.0 license | Copyright (c) by the authors | *DOI: https://doi.org/10.48084/etasr.5893*

ABSTRACT

The operating temperature of solid oxide fuel cells, oxygen division membranes, and oxygen sensors is determined by oxide-ion electrolytes. There is a strong incentive to reduce the operating temperature in solid oxide fuel cells, from 800°C to 500°C. The use of low-cost Na+ instead of K+ as dopant in monoclinic $SrSiO_3$ offers a wider solid solution range ($0.1<x< 0.5$) in $Sr_{1-x}Na_xSiO_{3-\delta}$ and obtains an oxide ion conductivity of 10^{-2} Scm^{-1} at 600°C, reducing the temperature of a smooth transition to full impairment of mobile oxide ions. For electrochemical characterization, the flat surfaces of the pellets were pasted with silver (Ag) paste and then sintered at 1200°C for 24 hours. The production of the $Na_2Si_2O_5$ phase was observed for most compositions due to thermal treatment. Crystallization of $Na_2Si_2O_5$ from glass was obtained in single-step calcination at 850°C after synthesis in an acetone medium, resulting in the highest conductivity. Although double calcination reduced conductivity, it improved thermal stability. Due to its low activation energy and lack of crystallization of other silicates, this material showed maximum conductivity after long-standing maturity at 600°C. Ethanol was used in place of acetone for powder assimilation and double calcination was also performed.

Keywords-solid oxide fuel cell; electrolyte; conductivity; activation energy, $SrSiO_3$

I. INTRODUCTION

Electrochemical energy conversion devices, such as Solid Oxide Fuel Cells (SOFCs), have been extensively studied as a potential technology for a wide range of applications, including large-scale stationary and portable power generators for both civilian and military applications [1]. The Yttria Stabilized Zirconia (YSZ) electrolyte used in conventional SOFCs has a suitable power density but also has the strong drawback of operating at high temperatures (~1000°C) [2]. On the other hand, high operating temperatures cause complicated difficulties for materials, such as the choice of materials and their chemical and physical compatibility with the restrictions of cell components for interconnects and seals, resulting in high cell manufacturing costs [2]. In this sense, the discovery of alternative electrolytes that can provide adequate performance in the so-called in-between temperature range of 500-700°C is one of the most crucial concerns for the widespread commercialization of SOFCs [3-4]. Several materials have been studied for intermediate temperature SOFCs, including doped ceria represented as oxide-ion conductors and $LaGaO_3$ and proton conductors signified by doped $BaCeO_3$ [4]. In addition to these oxides, doped strontium silicate with the general formula $Sr_{1-x}A_xMO_{3-\delta}$ (A = Na, K and M=Si/Ge) has attracted a lot of attention for its highest oxygen ion conductivity [5-7]. The main reason for the conductivity in $Sr_{1-x}Na_xSiO_3$ is that Na doping in $SrSiO_3$ forms oxygen vacancies through which oxygen ion flows [8-9]. As evidenced by NMR spectroscopy, due to the steric pause of large Sr^{2+} and Na^+ ions, conductivity was related to the development of the oxygen opportunity without changing the composition of $SrSiO_3$ [8]. Oxygen ions, which normally promote conduction, are not present in rare-earth oxyapatites. Several studies challenged these conclusions by highlighting the crucial role that glassy phases play in the Na_2O-SiO_2 system [6-9]. Specifically, conduction in $Sr_{1-x}Na_XSiO_3$ (SNS) due to Na^+ ion movement in the amorphous phase was observed by solid-state NMR spectroscopy investigations [10-11], and X-Ray Diffraction (XRD) analysis revealed constrained doping of Na in $SrSiO_3$ [12-13]. Conductivity appeared to be significantly affected by the crystallization of $Na_2Si_2O_5$ after some processing at approximately 650°C [12-13]. Some studies described how the amalgamation process and processing situations affect the structure and conducting qualities of alkali-doped $SrSiO_3$ and $SrGeO_3$ [14]. In large amounts, most of the materials investigated were made by a traditional solid-state method that involved mixing silica with acetone Na and Sr carbonates [12-14]. Spark Plasma Sintered (SPS) powders generated using the solid-state method create single-phase materials with tiny grains and strong ionic conductivity [15]. This study demonstrated that processing, in particular precursor reaction conditions and thermal properties, must have a major impact on phase composition and, subsequently, electrical properties. So, this study used a solid-state reaction to create $Sr_{1-x}Na_xSiO_3$ (x = 0.0 and 0.45).

II. EXPERIMENTAL PART

The solid-state reaction method approach was used to create powders of $Sr_{1-x}Na_xSiO_3$ (x=0.0 and 0.45), indicated as SNS. Wet ball milling with zirconia balls combined stoichiometric quantities of Sr and Na carbonates and nanometric SiO_2 in ceramic jars. To investigate the effects of solvent on Na inclusion and glassy phase development, three dissimilar dispersion media with growing polarity, acetone C_3H_6O, ethanol C_2H_6O, and distilled water H_2O, were used. Slurries were stored at 4°C after 24 hours of milling to acquire the final reaction result, and then the dry particles were sieved and heated to high temperatures in the air. The final product was produced by:

$$(1-x)SrCO_3 + \frac{x}{2}Na_2CO_3 + SiO_2 \rightarrow Sr_{1-x}Na_xSiO_{3-x/2} + \left(1-\frac{x}{2}\right)CO_2 \quad (1)$$

The composition with the highest conductivity for only x = 0.0 and x = 0.45 [2] was made with ethanol and water. Additionally, all compositions were "aged" in the air for 24 hours at 1200°C to further confirm their stability and to permit the crystallization or devitrification of any glassy phase. The powders obtained were compacted into pellets for conductivity testing that were generally 0.2 cm thick and 1 cm in diameter. Powder XRD with a Philips X'pert diffractometer (Cu K_α-radiation = 1.5418 Å) with Bragg Brentano reflection geometry seemed to verify its chemical phase purity. SEM was used to study the microstructures (shape and surfaces) of the powder and pellets at an accelerating voltage of 20 kV (JEOL, JSM-5610). The composition and apparent regularity of the compounds were confirmed by Energy-Dispersive X-ray (EDX) spectroscopy using a probe connected to the SEM. The samples were heated at a rate of 2°C/min while subjected to Thermo-Gravimetric Analysis (TGA) in an air atmosphere (airflow: 20 cm^3/min). Oxide ion conductivity was measured in an ambient atmosphere using a Solartron impedance analyzer (model 1287) with two probes at frequencies between 1 Hz and 10 MHz and an AC amplitude of 10 mV. Two Pt-blocking electrodes were produced by coating Pt paste (from Heraeus) over the two faces of the pellets and firing them for an hour at 800 °C. All measurements were taken at temperatures ranging from 300 to 800°C. To estimate the intercept to the real Z′ axis of a low-frequency semicircle, conductivity was calculated by extrapolating the difference between the source and the extrapolation of the intercept to the real Z′ axis.

III. RESULTS AND DISCUSSION

Figure 1 shows the XRD patterns of $SrSiO_3$ and $Sr_{0.55}Na_{0.45}SiO_3$ at ambient temperature. Both materials are monoclinic with a single-phase structure [16]. A high temperature (~1100°C) is needed for the parent $SrSiO_3$ to eliminate impurities such as Sr_2SiO_4 and SiO_2 and produce the single phase. The presence of voids is indicated by the broad flat top at 2θ~ (12-17°) for $SrSiO_3$. However, for $Sr_{0.55}Na_{0.45}SiO_3$, these flat tops become peaks. Peak splitting is observed for $Sr_{0.55}Na_{0.45}SiO_3$ at higher 2θ>40°, due to a disorder imposed on the parent $SrSiO_3$ [16]. The disorder in Na doping into $SrSiO_3$ may be due to stress and vacancy formation. In $Sr_{0.55}Na_{0.45}SiO_3$, the monoclinic phase formation is controlled by both the SiO_2 layers and the amorphous SiO_2 matrix, as opposed to $SrSiO_3$ where only the SiO_2 layers regulate the monoclinic phase growth [16]. EDX was used to examine the formulations of the $Sr_{1-x}A_xSiO_{3-\delta}$ (A = Na). Figure 2 shows SEM micrographs and Figure 3 shows the EDX profile of $Sr_{0.55}Na_{0.45}SiO_{3-\delta}$.

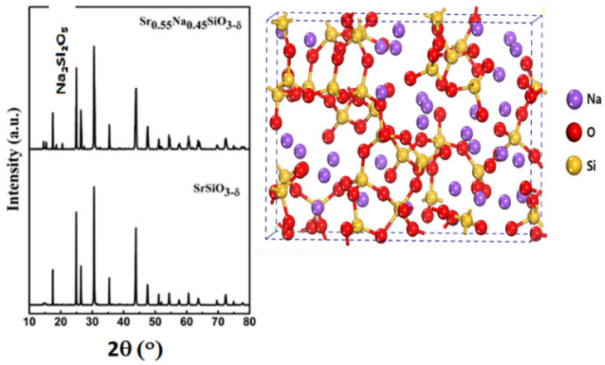

Fig. 1. XRD pattern of $SrSiO_3$ (with structure) and $Sr_{55}Na_{0.45}SiO_{3-\delta}$.

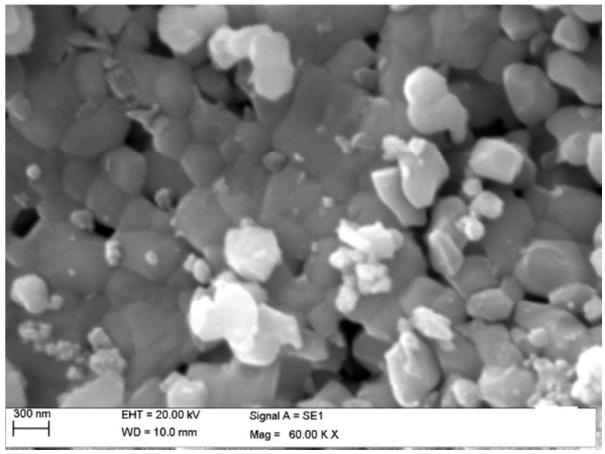

Fig. 2. FE-SEM image of $Sr_{0.55}Na_{0.45}SiO_{3-\delta}$.

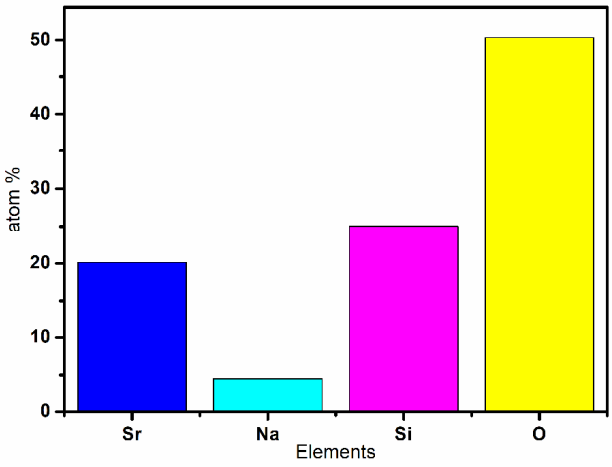

Fig. 3. EDX plot of $Sr_{0.55}Na_{0.45}SiO_{3-\delta}$.

The SEM analysis demonstrated the dense structure of the grains that ranged in size from 5 to 10 µm. On the other hand, the grains were in good contact due to the well-sintered pellets. The EDX analysis, shown in Figure 3, confirms the composition and superficial homogeneity (on the surface, not deep) of the material. The Archimedean principle produced pellets with a density of 97% of the theoretical density of the substance in water. It is difficult to estimate the oxide ion conductivity of the undoped sample, as $SrSiO_3$ is an electrical insulator within the measured temperature range and the conductivity is not due to the doped $SrSiO_3$ but due to the Na-rich phase ($Na_2Si_2O_5$). Figure 4 shows the complex impedance spectra of $Sr_{0.55}Na_{0.45}SiO_{3-\delta}$ at various temperatures. The bulk and grain boundary response was reflected in an apparent semicircle at high frequencies, while the electrode response was reflected in an apparent semicircular with a spike at low frequencies [17-18]. Total conductivity and not individual responses can be measured from bulk and grain boundaries if there are no clearly defined high-frequency semicircles [19]. Due to the high density of the pellet, the lack of a semicircle at high frequencies suggests that the contribution of the relative grain boundary to the resistance is almost minimal at high temperatures, as shown in Figure 4 [20-21]. The intercept of the low-frequency semicircle or the spike on the real (Z') axis is used to represent the bulk crystal conductivity in the spectrum in the non-appearance of a high-frequency semicircle [22]. The investigated system $Sr_{1-x}Na_xSiO_{3-\delta}$, for $x = 0.45$, achieved conductivity $\sigma \geq 10^{-2}$ Scm^{-1} at a lower temperature than $Sr_{1-x}K_xSi_{1-y}Ge_yO_{3-\delta}$ by shifting a smooth variation in activation energy centered at 550°C in $Sr_{0.8}K_{0.2}Si_{0.5}Ge_{0.5}O_{3-\delta}$ to a slightly lower temperature [22].

The potential for protonic conduction was expected in the investigated electrolytes due to the existence of absorbed water or hydroxide content, which was revealed by TGA measurement [16]. Figure 5 shows the TGA plots of $Sr_{0.55}Na_{0.45}SiO_{3-\delta}$. $Sr_{0.55}Na_{0.45}SiO_{3-\delta}$ had a negligible weight decrease at 400°C, possibly due to the vaporization of the adsorbed water.

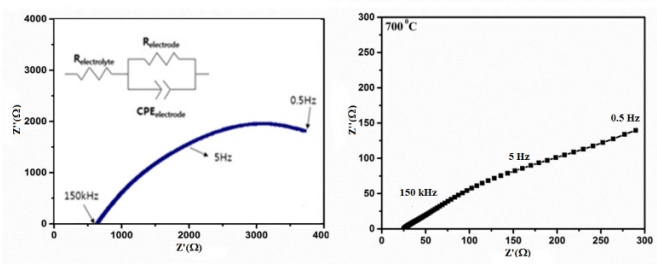

Fig. 4. Impedance plot of $Sr_{0.55}Na_{0.45}SiO_{3-\delta}$ at 500 (with electrical circuit) and 700°C.

The lack of weight loss at high temperatures (~ 400°C) due to the loss of lattice oxygen may be responsible for the improved electrical conductivity. Ions from absorbed water strongly approve the absence of any protonic conductivity at 400°C in the sample. However, it was unclear whether oxygen vacancies existed in the lattice or whether the sample $Sr_{0.55}Na_{0.45}SiO_{3-\delta}$ produced oxygen interstitials since there was little or no water adsorption. Glass transition and glass melting features are absent in $SrSiO_3$ and glassy phase formation in Na-doped $SrSiO_3$. When it formed, other phases such as Sr_2SiO_4 and SiO_2 were always present, proving that it is impossible to create pure oxygen-stoichiometric $SrSiO_3$ in a single monoclinic phase [23]. The overall conductivity of the system can be calculated as the sum of Na+ conduction in the glassy phases in the strontium sodium silicate. It is impossible to say whether the $Sr_{0.55}Na_{0.45}SiO_{3-\delta}$ or glass contributes more to conduction in the sample. Separation of two contributions is not possible in impedance diagrams because only one semicircle is present, and an additional investigation using different methods would be necessary to clarify this characteristic. Table I shows the conductivity and activation energy of similar studies [23-25].

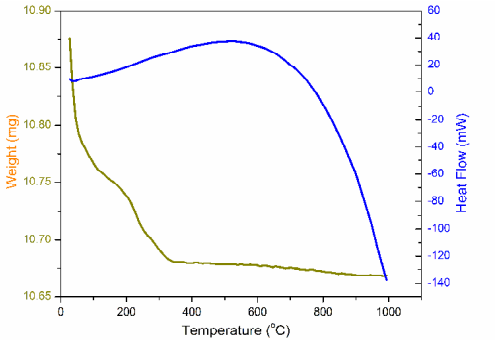

Fig. 5. TGA plot of $Sr_{0.55}Na_{0.45}SiO_{3-\delta}$.

TABLE I. COMPARATIVE STUDY OF CONDUCTIVITY AND ACTIVATION ENERGY

Sample	σ Scm^{-1} at 700°C	Activation energy (E_a) in eV
$SrSiO_3$	1.5×10^{-3}	0.35
$Sr_{0.6}Na_{0.4}SiO_3$	$(1.4\text{-}6.3) \times 10^{-3}$	(0.16-0.49)
$La_{0.9}Ba_{0.1}InO_3$	3.0×10^{-3}	0.88
$La_{0.9}Ca_{0.1}InO_3$	1.6×10^{-3}	0.81

Figures 6 and 7 show the variation of conductivity with temperature, indicating its dependence. Conductivity increases as temperature rises, showing that the movement of oxygen ion vacancies is speeding up [26-28]. The following equation was used to determine conductivity:

$$\sigma = \frac{t}{RA} \quad (2)$$

where t is thickness, A is the area, and R is the resistance of the pellet.

As can be observed, the experimental data and the recorded temperatures are nicely matched by a straight line [27-29], implying that the Arrhenius formula can be used to express conductivity:

$$\sigma = (\sigma_0/T)\, exp(-Ea/k_BT) \quad (3)$$

where E_a is the activation energy, k_B is Boltzmann's constant, and σ_0 is the pre-exponential factor.

Comparing the results of this study with [30], the observed conductivity is lower in this study. The same disparity was found in [31-33]. $Sr_{0.55}Na_{0.45}SiO_3$ has an activation energy of

0.39 eV and its conductivity at 700°C is higher (1.73×10^{-2} Scm^{-1}) than that of other solid electrolytes such as $La_{0.9}Sr_{0.1}In_{0.8}Mg_{0.2}O_3$ (10^{-3} Scm^{-1}), $La_{0.9}K_{0.1}Ga_{0.9}Mg_{0.1}O_3$ (7.65×10^{-3} Scm^{-1}), and $La_{0.9}Ca_{0.1}InO_3$ (1.6×10^{-3} Scm^{-1}) [34-38]. Finally, it can be concluded that $Sr_{0.55}Na_{0.45}SiO_3$ is a low-cost, rare-earth-free composite system, with a Na-rich amorphous phase ($Na_2Si_2O_5$) in the grain and Na-$SrSiO_3$ along the grain borders.

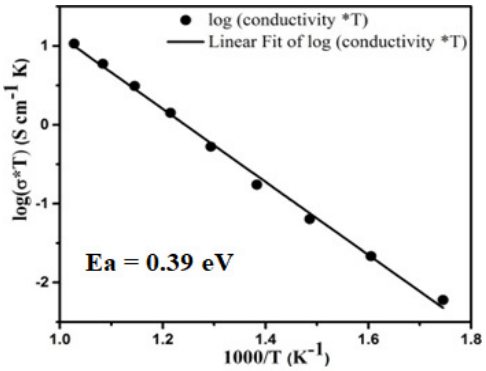

Fig. 6. Arrhenius plot for $Sr_{55}Na_{0.45}SiO_{3-\delta}$ conductivity.

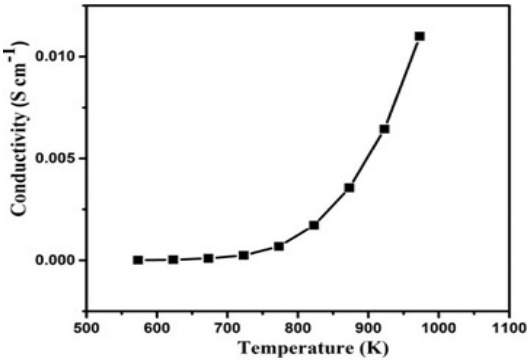

Fig. 7. Conductivity variation of $Sr_{0.55}Na_{0.45}SiO_{3-\delta}$ with temperature.

IV. CONCLUSION

In this study, $SrSiO_3$ and $Sr_{0.55}Na_{0.45}SiO_3$ were produced using solid-state processes. $SrSiO_3$ acts as an insulator over the temperature range studied, and $Sr_{0.55}Na_{0.45}SiO_3$ has strong ionic conductivity. XRD and SEM studies revealed that there are two phases in $Sr_{0.55}Na_{0.45}SiO_3$: intragrain SrSiO3 and intergrain $Na_2Si_2O_5$. TGA indicated that glass transition and glass melting features were absent in $SrSiO_3$ and glassy phase formation in Na-doped $SrSiO_3$. FE-SEM confirmed the presence of $Na_2Si_2O_5$, which is the main cause of the improved electric characteristics of $Sr_{0.55}Na_{0.45}SiO_3$. The electrical conductivity of this system was caused by the movement of charge carriers with grain boundaries. Therefore, this study concludes that $Sr_{0.55}Na_{0.45}SiO_3$ could be used as a suitable electrolyte material for IT-SOFCs.

ACKNOWLEDGMENT

This work was funded by the Deanship of Scientific Research (DSR), University of Jeddah, Saudi Arabia, under Grant No. UJ-21-DR-126. The author acknowledges the University for technical and financial support and the Indian Institute of Technology, Kanpur, India, for providing experimental facilities.

REFERENCES

[1] M. K. Mahapatra and P. Singh, "Chapter 24 - Fuel Cells: Energy Conversion Technology," in *Future Energy*, 2nd ed. T. M. Letcher, Ed. Boston, MA, USA: Elsevier, 2014, pp. 511–547.

[2] Z. Zakaria, S. H. Abu Hassan, N. Shaari, A. Z. Yahaya, and Y. Boon Kar, "A review on recent status and challenges of yttria stabilized zirconia modification to lowering the temperature of solid oxide fuel cells operation," *International Journal of Energy Research*, vol. 44, no. 2, pp. 631–650, 2020, https://doi.org/10.1002/er.4944.

[3] A. Aguadero *et al.*, "Materials development for intermediate-temperature solid oxide electrochemical devices," *Journal of Materials Science*, vol. 47, no. 9, pp. 3925–3948, May 2012, https://doi.org/10.1007/s10853-011-6213-1.

[4] J. A. Kilner and M. Burriel, "Materials for Intermediate-Temperature Solid-Oxide Fuel Cells," *Annual Review of Materials Research*, vol. 44, no. 1, pp. 365–393, 2014, https://doi.org/10.1146/annurev-matsci-070813-113426.

[5] K. Huang and J. B. Goodenough, *Solid Oxide Fuel Cell Technology: Principles, Performance and Operations*. Cambridge, UK: Woodhead Publishing, 2009.

[6] J. B. Goodenough, "Oxide-Ion Electrolytes," *Annual Review of Materials Research*, vol. 33, no. 1, pp. 91–128, 2003, https://doi.org/10.1146/annurev.matsci.33.022802.091651.

[7] A. C. Kundur, M. P. Singh, and V. A. Sethuraman, "Sodium Doped Strontium Silicates as Electrolyte for Intermediate Temperature Solid Oxide Fuel Cells," *ECS Transactions*, vol. 78, no. 1, pp. 467-475, May 2017, https://doi.org/10.1149/07801.0467ecst.

[8] L. Fan, "Solid-State Electrolytes for SOFC," in *Solid Oxide Fuel Cells*, Hoboken, NJ, USA: John Wiley & Sons, Ltd, 2020, pp. 35–78.

[9] B. Zhu, R. Raza, L. Fan, and C. Sun, *Solid Oxide Fuel Cells: From Electrolyte-Based to Electrolyte-Free Devices*. Weinheim, Germany: Wiley-VCH, 2020.

[10] G. Chen *et al.*, "Hyperbranched polyether boosting ionic conductivity of polymer electrolytes for all-solid-state sodium ion batteries," *Chemical Engineering Journal*, vol. 394, Aug. 2020, Art. no. 124885, https://doi.org/10.1016/j.cej.2020.124885.

[11] P. L. Rao, B. Pahari, M. Shivanand, T. Shet, and K. V. Ramanathan, "NMR investigations unveil phase composition–property correlations in Sr0.55Na0.45SiO2.775 fast ion conductor," *Solid State Nuclear Magnetic Resonance*, vol. 84, pp. 204–209, Jul. 2017, https://doi.org/10.1016/j.ssnmr.2017.05.001.

[12] M. Viviani, A. Barbucci, M. P. Carpanese, R. Botter, D. Clematis, and S. Presto, "Ionic Conductivity of Na-doped SrSiO3," *Bulgarian Chemical Communications*, vol. 50, special issue D, pp. 55–61, 2018.

[13] Y. Jee, X. Zhao, X. Lei, and K. Huang, "Phase Relationship and Ionic Conductivity in Na–SrSiO3 Ionic Conductor," *Journal of the American Ceramic Society*, vol. 99, no. 1, pp. 324–331, 2016, https://doi.org/10.1111/jace.13925.

[14] J. Peet, "Oxide Ion Conductors for Energy Applications: Structure, Dynamics and Properties," Ph.D. dissertation, Durham University, Durham, UK, 2018.

[15] S. W. Baek, J. M. Lee, T. Y. Kim, M. S. Song, and Y. Park, "Garnet related lithium ion conductor processed by spark plasma sintering for all solid state batteries," *Journal of Power Sources*, vol. 249, pp. 197–206, Mar. 2014, https://doi.org/10.1016/j.jpowsour.2013.10.089.

[16] P. Singh and J. B. Goodenough, "Monoclinic $Sr_{1-x}Na_xSiO_{3-0.5x}$: New Superior Oxide Ion Electrolytes," *Journal of the American Chemical Society*, vol. 135, no. 27, pp. 10149–10154, Jul. 2013, https://doi.org/10.1021/ja4042737.

[17] F. Dkhilalli, S. Megdiche, K. Guidara, M. Rasheed, R. Barillé, and M. Megdiche, "AC conductivity evolution in bulk and grain boundary response of sodium tungstate Na2WO4," *Ionics*, vol. 24, no. 1, pp. 169–180, Jan. 2018, https://doi.org/10.1007/s11581-017-2193-8.

[18] N. Hirose and A. R. West, "Impedance Spectroscopy of Undoped $BaTiO_3$ Ceramics," *Journal of the American Ceramic Society*, vol. 79, no. 6, pp. 1633–1641, 1996, https://doi.org/10.1111/j.1151-2916.1996.tb08775.x.

[19] J. Maier, "On the Conductivity of Polycrystalline Materials," *Berichte der Bunsengesellschaft für physikalische Chemie*, vol. 90, no. 1, pp. 26–33, 1986, https://doi.org/10.1002/bbpc.19860900105.

[20] L. Zhang, F. Liu, K. Brinkman, K. L. Reifsnider, and A. V. Virkar, "A study of gadolinia-doped ceria electrolyte by electrochemical impedance spectroscopy," *Journal of Power Sources*, vol. 247, pp. 947–960, Feb. 2014, https://doi.org/10.1016/j.jpowsour.2013.09.036.

[21] S. Sharma, K. Shamim, A. Ranjan, R. Rai, P. Kumari, and S. Sinha, "Impedance and modulus spectroscopy characterization of lead free barium titanate ferroelectric ceramics," *Ceramics International*, vol. 41, no. 6, pp. 7713–7722, Jul. 2015, https://doi.org/10.1016/j.ceramint.2015.02.102.

[22] J. T. S. Irvine, D. C. Sinclair, and A. R. West, "Electroceramics: Characterization by Impedance Spectroscopy," *Advanced Materials*, vol. 2, no. 3, pp. 132–138, 1990, https://doi.org/10.1002/adma.19900020304.

[23] P. Ptáček, "Rare-earth Element-bearing Apatites and Oxyapatites," in *Apatites and their Synthetic Analogues - Synthesis, Structure, Properties and Applications*, Rijeka, Croatia: IntechOpen, 2016.

[24] A. Glukharev, O. Glumov, I. Smirnov, E. Boltynjuk, O. Kurapova, and V. Konakov, "Phase Formation and the Electrical Properties of YSZ/rGO Composite Ceramics Sintered Using Silicon Carbide Powder Bed," *Applied Sciences*, vol. 12, no. 1, Jan. 2022, Art. no. 190, https://doi.org/10.3390/app12010190.

[25] B. Mutnuri, "Thermal conductivity characterization of composite materials," MSc Thesis, West Virginia University, Morgantown, WV, USA, 2006.

[26] O. N. Verma, S. Singh, V. K. Singh, M. Najim, R. Pandey, and P. Singh, "Influence of Ba Doping on the Electrical Behaviour of $La_{0.9}Sr_{0.1}Al_{0.9}Mg_{0.1}O_{3-\delta}$ System for a Solid Electrolyte," *Journal of Electronic Materials*, vol. 50, no. 3, pp. 1010–1021, Mar. 2021, https://doi.org/10.1007/s11664-020-08653-2.

[27] E. Kendrick and P. R. Slater, "Investigation of the influence of oxygen content on the conductivities of Ba doped lanthanum germanate apatites," *Solid State Ionics*, vol. 179, no. 21, pp. 981–984, Sep. 2008, https://doi.org/10.1016/j.ssi.2007.11.014.

[28] O. N. Verma, P. A. Jha, A. Melkeri, and P. Singh, "A comparative study of aqueous tape and pellet of $(La_{0.89}Ba_{0.01})$ $Sr_{0.1}Al_{0.9}Mg_{0.1}O_{3-\delta}$ electrolyte material," *Physica B: Condensed Matter*, vol. 521, pp. 230–238, Sep. 2017, https://doi.org/10.1016/j.physb.2017.06.081.

[29] O. N. Verma, N. K. Singh, Raghvendra, and P. Singh, "Study of ion dynamics in lanthanum aluminate probed by conductivity spectroscopy," *RSC Advances*, vol. 5, no. 28, pp. 21614–21619, Feb. 2015, https://doi.org/10.1039/C5RA01146A.

[30] A. K. Singh, R. Singh, and D. R. Chaudhary, "Prediction of effective thermal conductivity of moist porous materials," *Journal of Physics D: Applied Physics*, vol. 23, no. 6, pp. 698-702, Mar. 1990, https://doi.org/10.1088/0022-3727/23/6/010.

[31] R. D. Bayliss, S. N. Cook, S. Fearn, J. A. Kilner, C. Greaves, and S. J. Skinner, "On the oxide ion conductivity of potassium doped strontium silicates," *Energy & Environmental Science*, vol. 7, no. 9, pp. 2999–3005, Aug. 2014, https://doi.org/10.1039/C4EE00734D.

[32] P. G. Bruce, J. Evans, and C. A. Vincent, "Conductivity and transference number measurements on polymer electrolytes," *Solid State Ionics*, vol. 28–30, pp. 918–922, Sep. 1988, https://doi.org/10.1016/0167-2738(88)90304-9.

[33] C. Tealdi, L. Malavasi, I. Uda, C. Ferrara, V. Berbenni, and P. Mustarelli, "Nature of conductivity in SrSiO 3 -based fast ion conductors," *Chemical Communications*, vol. 50, no. 94, pp. 14732–14735, 2014, https://doi.org/10.1039/C4CC07025A.

[34] R. Pandey *et al.*, "The effect of synthesis and thermal treatment on phase composition and ionic conductivity of Na-doped $SrSiO_3$," *Solid State Ionics*, vol. 314, pp. 172–177, Jan. 2018, https://doi.org/10.1016/j.ssi.2017.10.021.

[35] Y. Jee, X. Zhao, and K. Huang, "On the cause of conductivity degradation in sodium strontium silicate ionic conductor," *Chemical Communications*, vol. 51, no. 47, pp. 9640–9642, May 2015, https://doi.org/10.1039/C5CC02638E.

[36] M. Najim, "Electrical Behavior of Lanthanum Aluminate (LAO) and Gadolinium Doped Ceria (GDG) Composite Electrolyte for Electrochemical Devices," *Engineering, Technology & Applied Science Research*, vol. 13, no. 2, pp. 10232–10238, Apr. 2023, https://doi.org/10.48084/etasr.5472.

[37] M. F. Abdelkarim, L. S. Nasrat, S. M. Elkhodary, A. M. Soliman, A. M. Hassan, and S. H. Mansour, "Volume Resistivity and Mechanical Behavior of Epoxy Nanocomposite Materials," *Engineering, Technology & Applied Science Research*, vol. 5, no. 2, pp. 775–780, Apr. 2015, https://doi.org/10.48084/etasr.536.

[38] L. Madani, K. S. Belkhir, and S. Belkhiat, "Experimental Study of Electric and Dielectric Behavior of PVC Composites," *Engineering, Technology & Applied Science Research*, vol. 10, no. 1, pp. 5233–5236, Feb. 2020, https://doi.org/10.48084/etasr.3246.